Biomacromolecules

pubs.acs.org/Biomac

Article

Cogrinding Wood Fibers and Tannins: Surfactant Effects on the Interactions and Properties of Functional Films for Sustainable Packaging Materials

André L. Missio,[⊥] Bruno D. Mattos,[⊥] Caio G. Otoni,[⊥] Marina Gentil, Rodrigo Coldebella, Alexey Khakalo, Darci A. Gatto, and Orlando J. Rojas*

Cite This: *Biomacromolecules* 2020, 21, 1865−1874

Read Online

ACCESS | Metrics & More | Article Recommendations | Supporting Information

ABSTRACT: We report on the combination of cellulose nanofibrils (CNFs) and condensed tannins from *Acacia mearnsii* for the development of hybrid, functional films. The tannins are fractionated and concentrated in polyphenolics that are used for functional components in the hybrid materials. Cogrinding of wood fibers with the tannins in aqueous media allows simultaneous fiber deconstruction and *in situ* binding of tannins on the freshly exposed cellulosic surfaces. Hence, a tightly bound bicomponent system is produced, which is otherwise not possible if typical adsorption protocols are followed, mainly due to the extensive hydration typical of CNFs. A nonionic surfactant is used to tailor the cellulose−tannin interactions. The proposed strategy not only enables the incorporation of tannins with CNFs but also endows a high and prolonged antioxidant effect of films formed by filtration. Compared to tannin-free films, those carrying tannins are considerably more hydrophobic. In addition, they show selective absorption of ultraviolet light while maintaining optical transparency in the visible range. The proposed simple protocol for incorporating tannins and surfactants with CNFs is suitable to produce functional materials. This is possible by understanding associated interfacial phenomena in the context of sustainable materials within the concept of the circular bioeconomy.

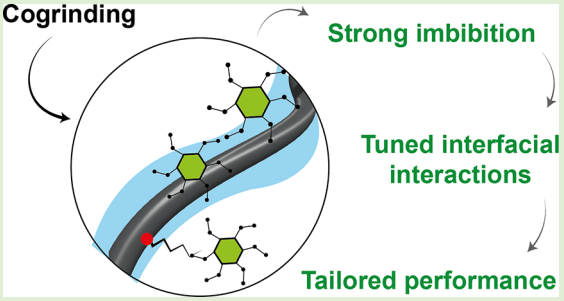

INTRODUCTION

Population growth and increased demands for foodstuff and goods are placing an increased pressure in the development of sustainable packaging materials. Such scenario is paralleled with environmental concerns arising from the use of plastics and nonrenewable polymers, particularly those for single-use applications.[1,2] Recyclability and biodegradability are increasingly recognized as part of the scientific and technological aspects within the emerging circular bioeconomy community. Additionally, packaging technologies are becoming critically important in the supply chain mostly to reduce losses driven by biotic and abiotic stresses; they are expected to provide increased stability and shelf life to systems that are prone to deleterious oxidative reactions, e.g., food, pharmaceuticals, cosmetics and bioactives, among others.[3,4] Therefore, packaging components not only should serve as a physical barrier (e.g. fluid and heat) but also should be able to alleviate oxidative stresses, e.g., as an antioxidant if activated with reactive oxygen species (ROS)- or free-radical-scavenging compounds.

Therein, plant-based building blocks are expected to play a critical role in the development of sustainable packaging solutions that aim to mitigate the carbon footprint of conventional plastics.[5] Nanocelluloses—e.g., cellulose nanofibrils and nanocrystals—feature the high potential to assemble in all-cellulose materials or in composites, all of which are expected to become a new generation of functional materials.[6] Nevertheless, nanocelluloses are especially attractive for large-scale applications due to the sustainable, renewable, and fast growing character of the plant biomasses used as raw materials for their production.[7] Active plant-derived molecules have been integrated with film-forming biopolymers to produce antioxidant packaging materials, including colloidal lignin particles,[8] lignin−carbohydrate complexes,[9] and tannin.[10,11] The latter, in particular, comprises a class of high-molecular-weight polyphenolics with well-documented antioxidant capabilities.[12] Although some efforts have been made for their isolation from byproducts in the food industry, condensed and hydrolyzable tannins are particularly relevant when isolated from forest-based biomass, i.e., to avoid competition with food sources.[13,14] Among the polyphenolic substances that are effective in providing antioxidant effects, commercial tannins are rather broad in composition. They comprise, in addition to ca. 70−75% condensed tannins, impurities such as sugars, organic acids, and gums.[15] The latter components reduce the specific

Special Issue: Anselme Payen Award Special Issue

Received: December 15, 2019
Revised: February 7, 2020
Published: February 10, 2020

antioxidant capacity of the system; therefore, tannin fractionation and purification may be necessary, especially if integrated in scalable processes. Approaches for their production can consider established processes used for lignin precipitation to obtain fractions of given molecular weight and phenolic content.[16] At the laboratory scale, Soxhlet-assisted solvent extraction (hexane, ethyl acetate, pentanol, propanol, and methanol) of tannins from Mimosa (black wattle; *Acacia mearnsii*) has been used for such a purpose.[17] Such a process allows the isolation of tannins into tailored molecular weight, phenolic content, and condensed tannin composition and associated antioxidant capacity. In fact, the properties of the respective fraction can be tailored based on the polarity of the solvent used for extraction. Thus, there is a great opportunity to engineer nanocellulose−tannin materials with tailorable properties. However, this demands the tannin−cellulose interactions to be better understood as far as their role during the processing and properties of the resulting materials.

In line with the concepts of circular bioeconomy and biorefinery, the present work aims at producing self-standing films comprising cellulose nanofibrils (CNFs) and tannin extracts as well as their use as a precursor for multifunctional hybrid films for packaging applications. We deepened the discussion on the embedding of tannin within a cellulose matrix that is easily obtained by cogrinding. The effects of such a system are further compared with the otherwise classic alternative of tannin addition to already formed CNF suspensions or films. We show that the interactions between tannin extracts and CNFs are enhanced by shear during the mechanical cogrinding, allowing for a finer control over their interactions, especially if surface-active species are used as aids. Our concept is rationalized based on the well-known behavior of surfactants at cellulosic interfaces.[18] In the present case, we build upon such a strategy to fine-tune the CNF−tannin interface, changing their interfacial interactions, and therefore their functional properties. Cogrinding all components, in the presence of a nonionic surfactant, is proposed here as a facile, mechanochemical route to tailor CNF−tannin interactions. Overall, we achieve control over the interactions of CNF with water as well as antioxidant action of the resulting self-standing hybrid films.

EXPERIMENTAL SECTION

Materials. Acetone (CAS no. 67-64-1; Sigma-Aldrich), 2,2′-azobis(2-amidinopropane) dihydrochloride (AAPH; CAS no. 2997-92-4; Sigma-Aldrich), 4-(1,1,3,3-tetramethylbutyl)phenyl-polyethylene glycol (Triton X-100; CAS no. 9002-93-1; Labsynth), 6-hydroxy-2,5,7,8-tetramethylchroman-2-carboxylic acid (Trolox; CAS no. 53188-07-1; Sigma-Aldrich), ethyl acetate (CAS no. 141-78-6; Sigma-Aldrich), monobasic and dibasic potassium phosphates (CAS no. 7778-77-0 and no. 7758-11-4; Vetec), poly(ethylene imine) (PEI; CAS no. 9002-98-6; Polysciences, Inc.), and sodium fluorescein (CAS no. 518-47-8; Sigma-Aldrich) were of analytical grade and used without further purification. Ultrapure Milli-Q water (Millipore Corp.) with a resistivity of 18.2 MΩ cm was used in all experiments, unless otherwise stated. Bleached Kraft pulp and tannin from *A. mearnsii* bark were provided by Suzano Papel e Celulose and SETA, respectively. The antioxidant capacity and the content of phenolic compounds and condensed tannins were determined following the methods described in the literature,[17] and reported in Table S1. Soxhlet-assisted fractionation was carried out as reported previously,[17] using 15 g of commercial tannin and 200 mL of either ethyl acetate or acetone for 6 h, followed by drying for 24 h and airtight storage in the dark.

Quartz Crystal Microgravimetry (QCM). Gold-coated Q-Sense sensors (Biolin Scientific) were cleaned with a UV-ozone ProCleaner instrument (BioForce Nanosciences, Inc.) for 15 min and spin-coated with PEI (0.33% w/v solution in water) and CNF (0.01 wt % aqueous suspension). The coated sensors were then dried at 80 °C for 10 min and allowed to equilibrate overnight in the QCM unit in water, before adsorption measurements. The change in frequency (3rd overtone) of the CNF-coated crystals was monitored over time with a Q-Sense E4 unit (Q-Sense AB) after injections of aqueous solutions of (i) tannin extracts (0.01 wt %); (ii) Triton X-100 (0.001 wt %); (iii) tannin extracts and Triton X-100, separately and in this order; and (iv) tannin extract and Triton X-100 together. Ultrapure water was used as the background solution.

Cogrinding of Cellulose Nanofibrils (CNFs), Surfactant, and Tannin Extracts. Cellulose pulp sheets were mechanically disintegrated into fluffy fibers using a high-shear vacuum homogenizer (model MH-100; Brogli & Co Basel Schweiz). A water slurry containing 1 wt % of fibers was prepared, and the tannin extracts were added at a 1:1 weight ratio (dry basis). An anionic surfactant, Triton X-100, was added to some of the samples (5 wt % based on dry solids). The amount of surfactant was determined based on literature values.[19] All formulations were then submitted to mechanical fibrillation with a friction grinder (Supermass-colloider, model MKCA6-2J; Masuko Sangyo Co., Ltd.) for 20−30 passes at 1500 rpm.

Film Formation. The CNF−tannin films (30 g m^{-2}) were produced through vacuum filtration, as detailed in our previous report,[11] with adaptations. Briefly, the respective aqueous colloidal dispersion was mixed in water (at ca. 1:15 weight ratio) and poured onto PTFE membranes (90 mm diameter, 0.22 μm pore size) connected to a vacuum filtration system. Wet films were dehydrated at room conditions, peeled off from the membrane, and equilibrated at 50% RH and 23 °C prior to testing.

Evaluation of Water Interactions and Structural, Spectroscopic, and Optical Properties. Rectangular films were submitted to a uniaxial tensile assay on a dynamic mechanical analyzer (DMA model Q800, TA Instruments) operating with an 18 N load cell and stretching rate of 1 N min^{-1} until rupture.

Film surfaces and cryofractured cross sections were gold-sputtered and imaged with a scanning electron microscopy (SEM, model VEGA-3SBU; Tescan Orsay Holding) using a 5 kV voltage. The optical transmittance profiles of the films were recorded at wavelengths ranging from 200 to 800 nm on a UV−vis spectrophotometer (model UV-2550; Shimadzu Co). The output was normalized by the film thickness as measured with a micrometer (resolution of 0.001 mm).

The contact angle (at least five per treatment) between the flat films and 20 μL water droplets was determined during 4 min through the sessile drop method using a drop shape analyzer (model DSA25; KRÜSS GmbH). The water vapor adsorption/desorption capacity of the films was assessed gravimetrically using dynamic vapor sorption (DVS) experiments at RH ranging from 0% to 95% and from 95% to 0% at 5% steps (DVS Intrinsic Plus, Surface Measurement Systems Ltd.). For isotherm plots, the subsequent stage started when the recorded weight varied less than 0.005% min^{-1} during a 10 min time frame—considering an initial dried weight of ca. 12 mg.

The water vapor transmission rates (WVTRs) of the films were determined gravimetrically by the "dry cup method" (ASTM-E-96 B). Briefly, films with a test area of 30 cm^2 were mounted in circular aluminum cups (68-3000 Vapometer EZ-Cups; Thwing-Albert Instrument Company) containing anhydrous $CaCL_2$ (0% relative humidity). Then, the samples were acclimated to 23 °C and 50% RH and weighed periodically until a constant rate of weight reduction was attained. The temperature and humidity of the chamber was controlled using a Climaveneta climate control system model AXO 10. The humidity gradient was the driving force for water molecules to diffuse within a material. Herein, a 50/0% relative humidity (RH) gradient was used. Water vapor permeability (WVP) was then obtained by multiplying the WVTR value by the sample thickness and then dividing the result by the water vapor difference across the film. All experiments were performed in triplicate.

Attenuated total reflectance Fourier-transform infrared (ATR-FTIR) spectra were acquired for tannin powders and films on a Spectrum Two instrument (PerkinElmer Inc.), at wavenumbers ranging from 500 to 4000 cm^{-1} (spectral resolution of 2 cm^{-1}, and accumulating 64 scans per sample). X-ray diffractograms were recorded

https://dx.doi.org/10.1021/acs.biomac.9b01733
Biomacromolecules 2020, 21, 1865−1874

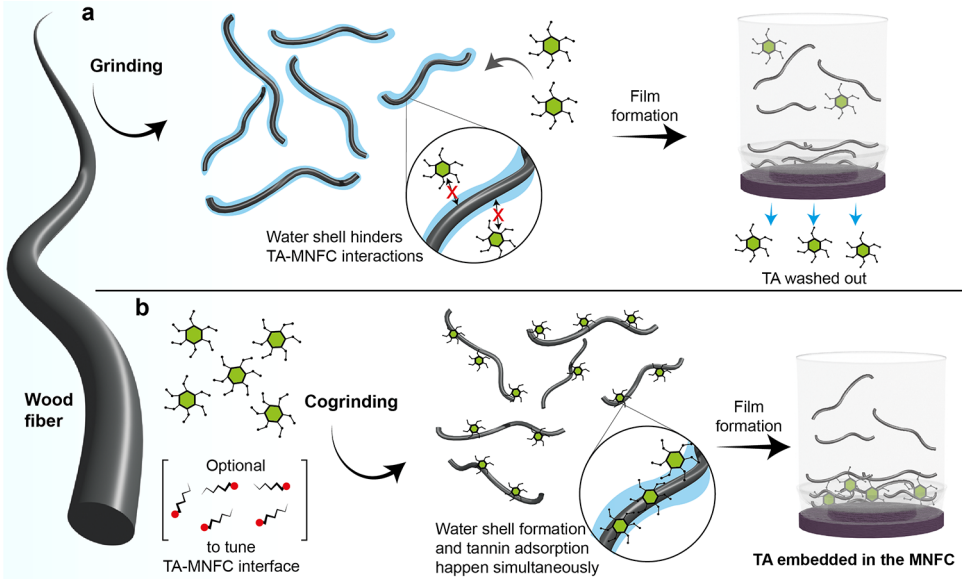

Figure 1. Schematic illustration of the cogrinding process proposed to effectively incorporate condensed tannins (CTs) in a CNF matrix suitable for the preparation of functional films. (a) Water molecules strongly bound to CNF surfaces hinder their interaction with tannins. (b) Cogrinding wood fibers with tannin molecules facilitates *in situ* binding between newly exposed CNF surfaces and tannins available in the aqueous medium during the defibrillation process. We exploit the competition between water−cellulose and cellulose−tannin interactions during cogrinding to produce films comprising the two components.

at Bragg angles (2θ) from 0° to 60° on a powder diffractometer (model X'Pert Alpha-1; PANalytical B. V.) operating with Cu Kα radiation, 45 kV voltage, and 40 mA current. The step size was 0.001°, and the counting time was 1 s per step. Films were sandwiched between a thin Mylar sheet and a zero-background Si disk and were rotated during the runs.

Antioxidant Assay. Each film (10 mg = ca. 15 × 15 mm^2) was immersed in 10 mL of water and changed periodically (after 1, 4, 6, 8, 12, 24, 36, and 48 h) to the same volume of fresh water. The release media were sampled as soon as the film was removed and analyzed as for their antioxidant capacities through the oxygen radical absorbance capacity (ORAC) method.[20] Potassium phosphate buffer (75 mmol L^{-1}) was used to dilute release medium samples (to 50 mg L^{-1}), and Trolox (4−98 μM) was used to build a standard curve. Aliquots (25 μL) of the release medium and Trolox solutions, as well as 150 μL of fluorescein (81 nmol L^{-1}), were added into a black 96-well microplate, which was then incubated at 37 °C for 10 min. Subsequently, 25 μL of 152 mmol L^{-1} AAPH solution as a peroxyl radical generator was added, and the fluorescence−excitation and emission at (485 ± 10) and (535 ± 20) nm, respectively, was read on a Sense microplate reader (Hidex Oy) with 120 measuring cycles during 120 min at 37 °C. The ORAC values were expressed as μmol Trolox equivalent per g of sample according to the area under the curve of fluorescence decay versus time, calculated as described in our previous report.[11] All experiments were performed in triplicate.

RESULTS AND DISCUSSION

Rationale for Fiber−Tannin Cogrinding. In contrast to hydrolyzable tannins that have a remarkable binding capacity with virtually any surface,[18,21] polymeric condensed tannins (M_w up to 4500) are less interactive. This is due to their relatively low free phenolic binding sites as well as steric hindrance arising from the tridimensional conformation of the macromolecular structures.[17] Therefore, incorporation of tannin condensed structures in cellulosic matrices, aiming at the formation of functional materials, is highly unfavorable. In fact, analogous amphiphilic macromolecules in the same molecular weight range did not adsorb onto cellulosic surfaces, but did onto lower-surface-energy films.[22] The involved interactions are further limited by the inherent highly polar nature of both tannins and celluloses, e.g., the hydration layer formed upon binding of water molecules at the interfaces. Therefore, the addition of tannin to an aqueous suspension of an already-prepared CNF suspension results in a weak cellulose−tannin interface. The expected tightly bound water layer formed on the cellulosic surfaces (known to form even in air at low humidity)[23,24] prevents interactions with tannins in aqueous media. Thus, losses of tannins occur upon filtration of an aqueous suspension containing CNF and tannins (close to null tannin retention in the resultant film) (Figure 1a).

Thus, to effectively promote tannin−cellulose interactions and to produce tannin-rich CNF films, a cogrinding process involving the precursor wood fibers and tannins, both dispersed in an aqueous medium, has been proposed.[11] During mechanical defibrillation, the hierarchical structure of wood fibers, with relatively low surface area, is disassembled into fibrils that expose new surfaces that rapidly interact with the surrounding water molecules to form a strong (bound water) layer. In the cogrinding approach, we enrich the aqueous medium with tannins to improve their interactions with the continually unraveling cellulosic surfaces, thereby competing with the formation of bound water. While the molecular nature of this process is to be investigated further, we provide indirect evidence of tannin binding with CNF throughout the cogrinding process, warranting CNF films with strongly embedded tannin molecules (Figure 1b). The cogrinding process yields tannin-loaded CNFs with average widths, that correlate directly with the diameter,[25] below 50 nm (Figure S1).

To obtain further control over tannin−cellulose interfaces, we added a small fraction of a nonionic surfactant to the precursor fiber−tannin suspension. The nature of the interactions between tannin and cellulose at the interfaces is expected to be dominated by H-bonding and π-interactions,[18] which result in exposed hydrophobic domains of condensed tannin structures, as the outer surface of the CNF. This resulted in a hydrophobic, modified CNF that is built from a superhydrophilic matrix

https://dx.doi.org/10.1021/acs.biomac.9b01733
Biomacromolecules 2020, 21, 1865−1874

(unmodified CNF) together with the water-soluble tannins. Interestingly, when the surfactant is incorporated in the system, the interplay between the components favors the interactions between the hydrophobic domains of the tannin and the hydrophilic cellulose. Another potential benefit of this approach is the enhanced penetration of tannins into the CNF matrix through the capillary structure of the CNF owing to the low surface energy of the surfactant solution.[26,27] The proposed protocol endows a unique opportunity to tailor the loading and release of antioxidant molecules as well as the wettability of CNF−tannin films, as discussed next.

Film Formation and Structural Properties. To gain further insights on the interactions between cellulose and tannin extracts as well as on the role of the nonionic surfactant on the tannin adsorption, model CNF films were prepared on the QCM sensors and exposed to the adsorbents (tannins and surfactant) while monitoring the resonance frequency over time (Figure 2).

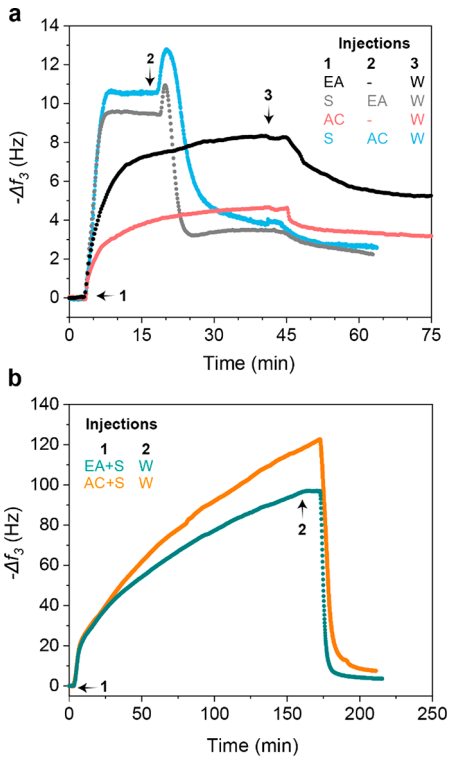

Figure 2. QCM frequency shift (3rd overtone, Δf_3) for CNF films deposited on the QCM sensor upon exposure to tannins extracted either with acetone (AC) or ethyl acetate (EA). Data for adsorption of a nonionic surfactant, Triton X-100 (S), are also included. The sensograms include data for (a) individualized addition or (b) combined addition. A washing step with the background solvent, water (W), is included at the end of the process. The respective injections are indicated by arrows placed on the corresponding time.

The shift in frequency to more negative values (increased $-\Delta f$), for all treatments, indicates an increased oscillating mass. The kinetics and extent of mass gain, however, are found to depend remarkably on the sequence of injection. The injection of the given tannin solution on CNF-coated sensors reveals a slow kinetic process with a relatively large gain in oscillating mass. After washing, only 37−30% of the frequency shift is restored compared to the mass before washing, revealing the extent of adsorption.

The injection of surfactant solution on the CNF-coated sensor leads to a large and rapid increase in the sensed mass (Figure 2a). We note, however, that such adsorption is highly reversible, as can be concluded from the fact that the frequency is extensively restored upon water rinsing (Figure S2a). This effect was found to be less pronounced at higher surfactant concentrations in a similar system.[28] Subsequent injection of tannin solution on the CNF-coated sensor carrying preadsorbed surfactant leads to a rapid and transient mass gain, an effect that is immediately reversed, revealing a mass loss, possibly due to desorption of the initially preadsorbed surfactant layer. Upon washing with water, the final mass gain is equivalent to 21−24% with respect to that before washing (Figure 2a). The results indicate that tannin adsorption and surfactant desorption are competing phenomena. What is more remarkable is that the oscillating mass profile is quite different when solutions of tannin—regardless of its extract (EA or AC)—containing the surfactant are injected simultaneously (Figure 2b): an initial fast adsorption is observed during the few minutes after injection (slope similar to that observed after injection of the single component surfactant solution), followed by a slower adsorption dynamic (slope closer to that of the adsorption of tannin only). Such behavior is even more pronounced for the acetone-extracted tannin/surfactant solution, which reaches an equilibrium after a longer period (Figure S2b). Although the change in frequency in this case is remarkably higher than that for the other conditions, washing with water almost fully removed any adsorbed mass (only 4−8% of effective mass is irreversibly adsorbed after washing). Despite the challenge of translating the QCM results to understand the phenomena occurring during cogrinding, the data point to the minimum adsorption of tannins on cellulose, and in fact, negligible adsorption occurs when tannin and surfactants are exposed to CNF surfaces. This is in contrast to a more efficient tannin retention after high-shear mechanochemical processing. With the cogrinding process, the concentration of tannins in the CNF matrix is over 13 wt %, for all films. This value represents the amount of tannin that could be extracted from the films until constant mass by using 1 M NaOH; however, a large amount of tannins clearly remained in the extracted films (as indicated by the brown color of the alkali-treated films). This corresponds to irreversibly adsorbed tannins. We propose that the main difference is that in the latter case tannins adsorb more effectively on freshly exposed cellulosic surfaces, as they develop during the grinding process.

As expected, the presence of tannins and/or surfactant does not affect the main microscale features of the CNF films obtained after grinding. SEM images (Figure 3) indicate densely structured fibril layers that align perpendicularly to the filtering direction, owing to their high aspect ratio. Similar features have been observed for other high-aspect-ratio nanocelluloses.[6,29,30] In general the films contain voids and pores; however, the morphology of the surfactant-containing films showed more discontinuities, which will likely affect the mechanical, barrier, and optical properties of the system, as will be discussed further.

The apparent crystallinity of the CNF films was not affected by the presence of tannin or surfactant (Figure S4), although a slight reduction in the calculated Segal crystallinity index, from 77% (neat CNF film) to 70−75% (tannin-containing films), was observed and ascribed to the presence of amorphous adsorbed tannin. The FTIR spectra—with [0, 1] normalization—of the tannin-containing films display the characteristic peaks observed for tannin fractions, especially at 2900 cm^{-1}, indicating C−H

https://dx.doi.org/10.1021/acs.biomac.9b01733
Biomacromolecules 2020, 21, 1865−1874

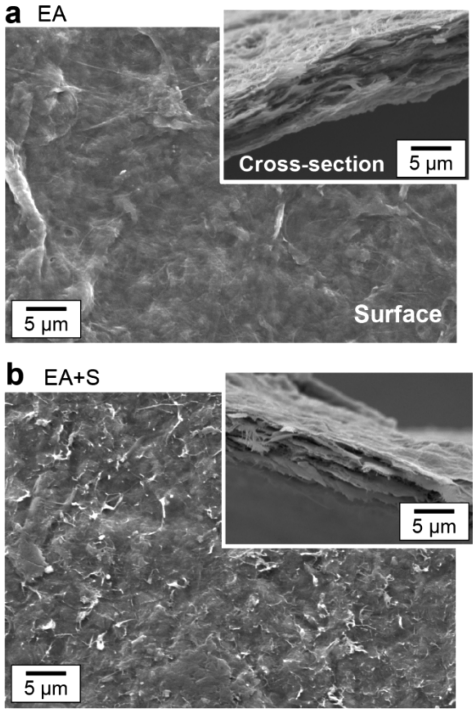

Figure 3. Representative surface and cross-sectional (insets) scanning electron micrographs of CNF-based films containing (a) ethyl acetate-extracted (EA) tannins and its combination with (b) the nonionic surfactant (EA+S). Films prepared from acetone-extracted tannins (AC and AC+S) displayed a similar morphology (see Figure S3).

stretching bonds, and at 1590 cm^{-1} that corresponds to the aromatic/phenolic vibrations from the polyphenolic macromolecule.[31] When compared to the respective controls, the absence of new peaks strongly indicates that supramolecular interactions (noncovalent) dominate the tannin−cellulose interface. From the FTIR spectrum of the EA tannins, a higher hydrophobicity of the system is expected, as indicated by higher intensity of C−H hydrophobic groups (Figure S5).

Physical−Mechanical Properties. The incorporation of tannin molecules within the CNF matrix led to a ca. 50% reduction in the ultimate tensile strength and stiffness of the films (Figure 4a−c). This is reasonable since better entanglement and interactions are expected in cellulosic materials derived from the transfer of supramolecular cohesion from the cellulose chains to the fibrils and their higher-order constructs. Upon tannin adsorption on the primary fibrils, cellulose−cellulose H-bonding is partially hindered at the nanoscale, limiting fibril−fibril interactions. We hypothesize that, in the presence of tannin, H-bonding and hydrophobic interactions play a role in the cohesion of the film; however, the load of tannins is low enough in such a way that significant interfibril interactions are preserved leading to cohesive bicomponent films. Finally, we note that if the tensile strength (Figure 4b) is normalized by film density, the resulting specific strength (Figure 4d) is higher in the presence of tannins. Logically, this is due to the relatively lower density of the respective films. Similar outcome as far as mechanical performance was reported for nanopapers of lignocellulose nanofibrils containing 0−14 wt %

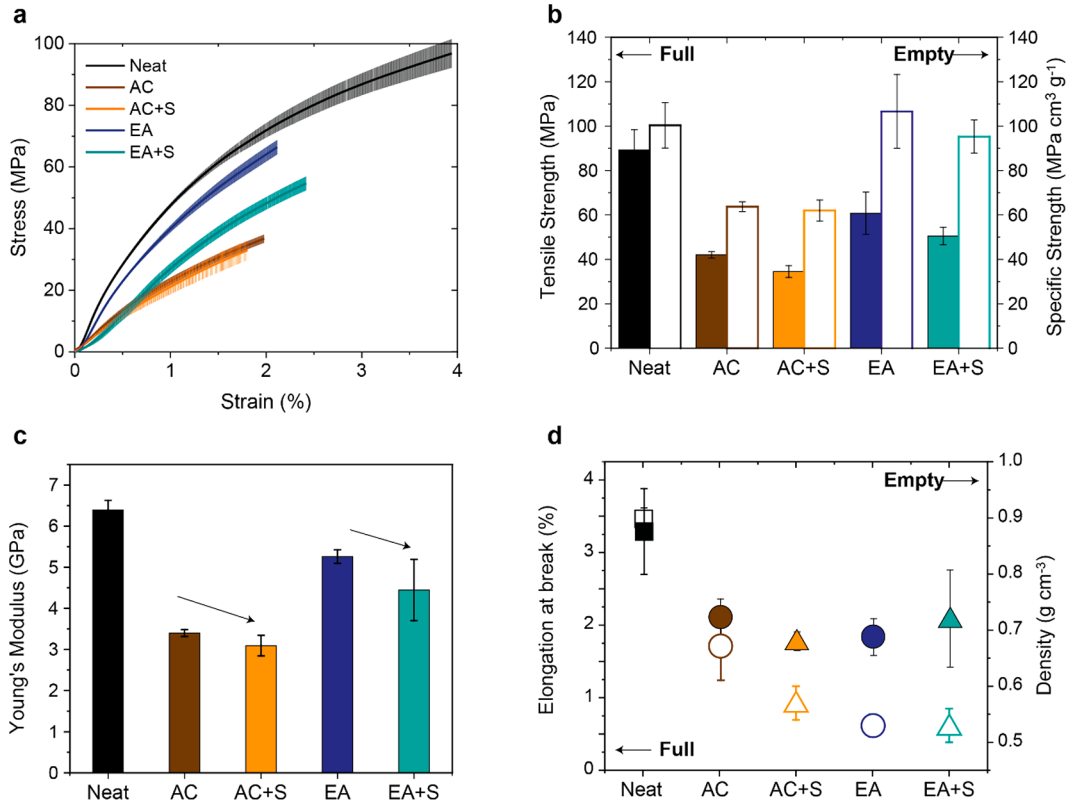

Figure 4. Mechanical properties of the CNF−tannin films displaying (a) typical engineering tensile stress−strain curves; (b) ultimate tensile strength and specific strength after normalization by film density; (c) Young's modulus; and (d) elongation at break and density of films based on CNF in the absence (Neat) or in the presence of acetate (AC)- or ethyl acetate-extracted (EA) tannins, either by themselves or in combination with the nonionic surfactant (AC+S and EA+S, respectively).

https://dx.doi.org/10.1021/acs.biomac.9b01733
Biomacromolecules 2020, 21, 1865−1874

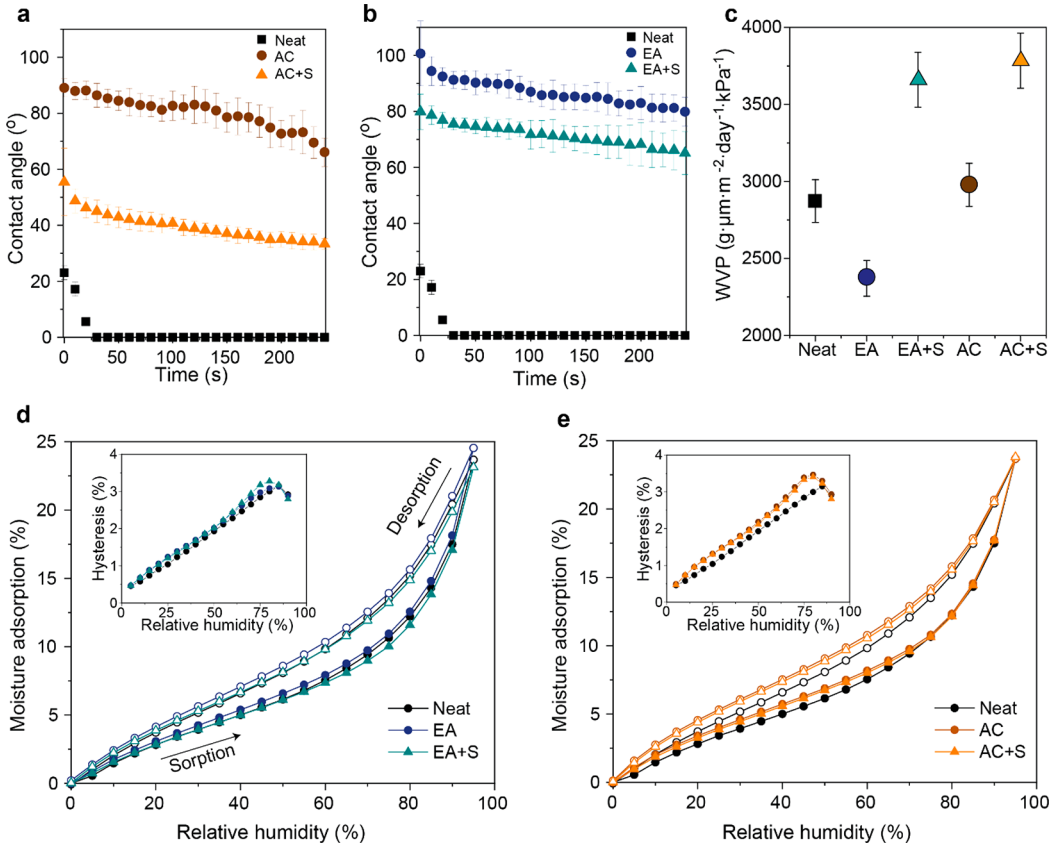

Figure 5. Apparent water contact angle of CNF films in the absence (Neat) and presence of (a) acetone (AC)- or (b) ethyl-acetate-extracted (EA) tannins. The contribution of nonionic surfactant is also observed (AC+S and EA+S). (c) Water vapor permeability (WVP) of the tannin-containing films. Also shown is the dynamic vapor sorption isotherms and relative hysteresis (insets) for (d) EA and EA+S and (e) AC and AC+S films, compared to those of neat CNF.

of residual lignin, another plant biomass-derived polyaromatic compound.[32]

Keeping in mind that the tannin loading is similar for all films (13 ± 1 wt %), compared to the AC-extract fraction, the strength of the film carrying EA-extracted tannin correlates with its more hydrophobic character and lower M_w. The adsorption of smaller tannin molecules on the CNF surface leads to a reduced steric hindrance when the fibrils approach each other during removal of water and consolidation of the dried film, thus favoring interfibril H-bonding. This is proposed as a main factor leading to the cohesion in the film. Formation of hydrophobic patches across the film is expected to take place, affecting the balance between hydrophobic interactions and H-bonding. The addition of the surfactant has a slightly negative effect on the tensile strength of the films as well as their stiffness (Figure 4a–c). The presence of surfactant causes further disruption of the tannin–fibril and interfibril hydrophilic interactions,[19] creating discontinuities at the interfaces and reducing the stress transfer mechanism across the fibrillar network.

Water Interactions. An important aspect from the point of view of self-standing films intended for packaging is the water interactions, especially relevant in systems involving CNFs as the main component. Associated aspects define the wettability, wet resilience, and barrier properties (water vapor). Most polysaccharides and their respective structures, such as CNFs, are highly hydrophilic and display a poor barrier to moisture.[33] Other properties can be compromised as well, including gas transport and mechanical strength, to mention a few.[33] Our CNF films presented an apparent water contact angle (WCA) of less than 25° as measured during the first seconds after placing a water droplet on the surface. Wicking produces unreliable data after 30 s, due to the highly hydrophilic nature of the films (Figure 5).

Remarkably, the presence of tannins in the CNF-based films leads to a significant increase in WCA (>90° for films containing ethyl acetate-extracted tannin, Figure 5b), which is maintained for a relatively long time (Figure S6). This is somehow unexpected considering the mixture of a hydrophilic biocolloid with a water-soluble molecule; however, related effects have been observed for CNF combined with other tannins[11] and chitosan.[34] The observed behavior results from the preferential polar interactions that dominate at the CNF–tannin interface, exposing the hydrophobic binding sites of tannin molecules, hence decreasing film wetting. The intermediate wetting behavior of the surfactant-containing films (Figure 5a,b) arises from its amphiphilic nature. In this case, tannin molecules interact with CNF (i) directly, through H-bonding—increasing surface hydrophobicity, as discussed above—and (ii) by having the surfactant acting as a spacer, i.e., with the surfactant's polar head interacting with the hydrophilic groups of CNF and exposing the nonpolar tails to tannin's hydrophobic groups—exposing its hydrophilic domains.

The CNF films containing tannins behave differently in terms of water vapor permeability (WVP). When compared to the neat CNF film, those containing the acetone extract increased the WVP. However, a decrease in WVP was observed for the film containing the ethyl acetate extract. Disruptions on the packed fibrillar CNF structure caused by tannin molecules are likely

https://dx.doi.org/10.1021/acs.biomac.9b01733
Biomacromolecules 2020, 21, 1865–1874

reasons for the increased WVP. On the other hand, the hydrophobicity of the tannins, when adsorbed on the fibril surfaces, are expected to decrease the WVP. Therefore, for films containing the ethyl acetate (EA) tannin extract, the hydrophobicity effect dominated over that related to morphology. As discussed earlier, EA extract possesses a significantly more hydrophobic character when compared to the AC extract. The addition of surfactant led to a remarkable increase in WVP, for both cases, which is in line with the results related to water interaction discussed so far (Figure 5c).

Interestingly, the films behave similarly and independently of composition as far as adsorption and desorption of water vapor (Figure 5d,e). The equilibrium moisture content at 95% RH ranges from 23% to 25% and does not follow any clear trend. All sorption isotherms are sigmoidal in shape, which is typical of cellulosic materials due to the adsorption of water molecules as a monolayer at low RH, followed by multilayer-induced swelling at intermediate RH values, and water condensation in capillaries and pores at high RH.[35] This outcome is a clear manifestation of how differently materials behave as far as water interactions as assessed by short-term experiments with liquid moisture (e.g., water contact angle) and longer-term experiments with water vapor (e.g., sorption isotherms).

Antioxidant Capacity. The role played by (poly)phenolic compounds—including condensed and hydrolyzable tannins—on oxidative processes has been demonstrated to result from their ability to prevent or delay the formation of free radicals (e.g., by chelating pro-oxidant ions) or the propagation of related reactions (e.g., by quenching peroxyl radicals).[12] The combination of tannins with film-forming matrices can be used as a strategy to produce antioxidant packaging materials.[11] Herein, we measured the antioxidant capacity of the tannin molecules leached out from the films after immersion in water during given times (Figure 6). With such a method we evaluated the radical scavenging capacity of the films under the harshest possible environment conditions, in terms of oxidation and in the context of packaging applications. Although peroxyl radicals may arise from atmospheric oxygen, a minimum water content is often required for developing significant oxidative stresses. Higher antioxidant capacity was observed for the EA and AC extracts, obtained by solvent fractionation, when compared with the native tannin (Table S1). This, aligned with the addition of surfactant to tailor the CNF−tannin interactions, resulted in high and adjustable antioxidant capacity of the films (Figure 6).

As expected, no detectable antioxidant activity was measured for water, surfactant, nor the neat CNF films. The leachates from the tannin-embedded CNF films, contrastingly, were effective as antioxidants (Figure 6). Because the water containing the tannin leachates was replaced by fresh water, at every measuring time point, the concentration gradient of antioxidant molecules decreases over time. Accordingly, the antioxidant capacity of all films decreases asymptotically with time. The rate at which the tannin molecules leach out from the films differed among the treatments. Tannin molecules leached out more extensively—rate and amount—from the surfactant-containing films owing to the weakened tannin−cellulose interaction. Such leaching effects produced by surfactants in fiber systems have been discussed in our earlier publication, in the context of surface activity.[36] Relevant to this study, however, is that a more extended antioxidant action is observed in the presence of surfactant. After 12 h of immersion in water, the leachate from the EA+S films presents a 3-fold higher antioxidant action compared to that of surfactant-free counterpart.

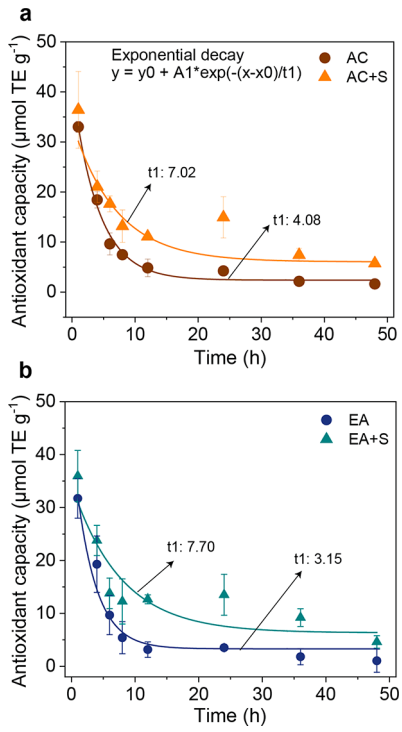

Figure 6. Oxygen radical absorbance capacities, expressed as Trolox equivalents (TE), of aqueous leachates from CNF films obtained after cogrinding with (a) acetone-extracted tannins in the presence (AC+S) or absence (AC) of surfactant. The case of (b) ethyl acetate-extracted tannins with (EA+S) or without (EA) surfactant is also illustrated. The data include standard deviation bars and fits to an exponential decay model with determination coefficients (r^2) > 0.9.

UV-Shielding. Compounds or particles that absorb or scatter light are promising candidates for functional packaging due to their ability to decrease light transmittance[8] as we have previously demonstrated for lignin-containing films or coatings.[37] A dual-action approach is therefore possible for films containing tannins that can act as both antioxidant (Figure 6) and photoprotective agent (Figure 7). Thus, reduced oxidation is expected as a result of the decreased transparency to ultraviolet and visible radiations.

Figure 7a indicates the efficiency of CNF−tannin films in blocking, to different extents, the passage of light in the full UV−vis spectrum. Neat CNF films scatter light due to the shift in the refractive index at the air−cellulose interface.[38] This is especially true when the fibrillar network is formed by polydisperse coarse nanofibers,[30] as in the case of the unfractionated CNFs typically obtained from mechanical fibrillation. Another prerequisite for light to be scattered is that the scattering domains are larger than the wavelength of the incident radiation, a reason why the transmittance is lower in the UV region, regardless the composition of the film (Figure 7a−c). However, there is a clear enhancement of the photoprotection by tannin-containing films, which is ascribed to their strong UV-absorbing capacity (Figure 7d). Indeed, the valley centered at ca. 270−280 nm is a tannin fingerprint, where the absorbance is maximized.[39] The UV-shielding introduced by tannins is particularly relevant in the context of light-catalyzed reactions. This is because systems that are prone to photo oxidation are more sensitive to UV radiation due to its higher quantum energy.[40] This interesting feature of the tannin-containing CNF films can be easily tuned by increasing the film thickness (Figure 7c), which can be

https://dx.doi.org/10.1021/acs.biomac.9b01733
Biomacromolecules 2020, 21, 1865−1874

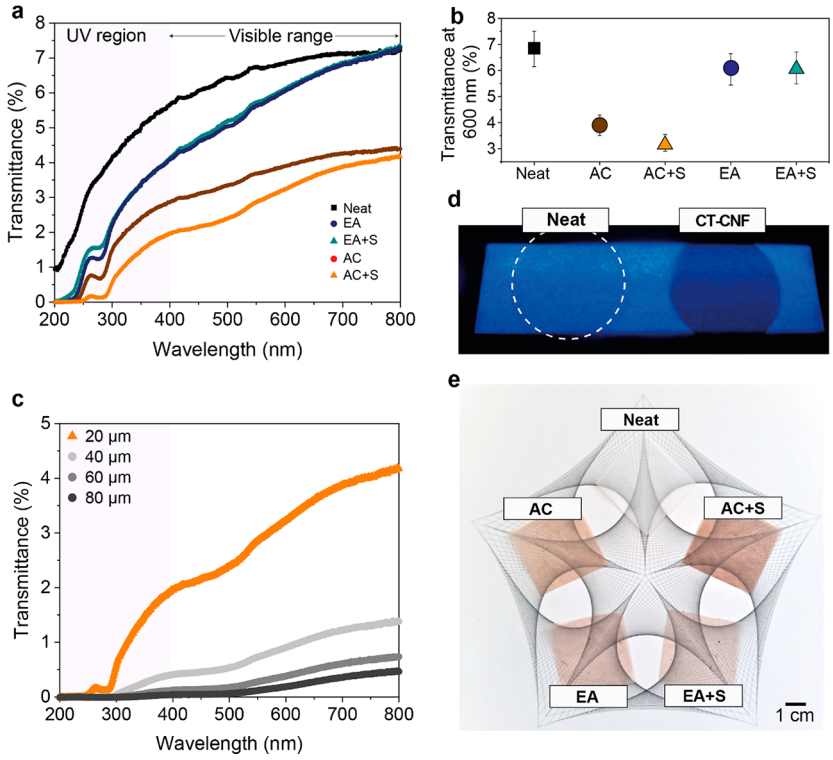

Figure 7. Light transmittance (a) profiles in the ultraviolet (UV) region and visible range as well as (b) values for transmittance at 600 nm. 20 μm thick CNF films in the presence or absence (Neat) of acetone (AC)- or ethyl acetate-extracted (EA) tannins, combined or not with an anionic surfactant (AC+S and EA+S, respectively) were used. (c) Transmittance profiles within the UV−vis range for AC+S films of different thicknesses. (d) Representative tannin-free and tannin-containing CNF films (20 μm in thickness) on top of a 366 nm light source, illustrating the UV-shielding introduced by the tannin extract. (e) Images of all films produced in this study under visible light, making evident their transparency and haziness.

exploited for a near total blockage of the radiation (UV to the lower visible range), as seen in AC+S films of >40 μm in thickness. From Figure S7, for the optical transmittances of 60 μm thick neat and AC+S films, it becomes evident that such behavior is enabled by tannin chromophores. Interestingly, the limited transmittance does not negatively affect the clear appearance of the films (Figure 7e), which is assigned to the rather low haziness upon tannin incorporation.[10]

CONCLUSIONS

Antioxidant films with high UV-shielding character were produced by combining cellulose nanofibrils with condensed tannins through a cogrinding process. A trade-off is expected for the mechanical and functional properties, for example, by optimizing the amount of tannins in the precursor's suspensions prior to consolidation into films. The addition of a nonionic surfactant provided further control over the tannin−cellulose interface and therefore on the film properties. Higher hydrophobic character, indicated by increased water contact angles, was obtained in the tannin-containing films when compared to the neat CNF counterpart. Wettability of the films could be tuned by the addition of surfactant. While not impairing the specific physical−mechanical properties of CNF films, tannin extracts added antioxidant and UV-shielding functionality. The surfactant played a major role by boosting the release of the polyphenolic compounds, prolonging the antioxidant effect of the films. This contribution adds to the growing literature on functional nanocellulose−tannin films by demonstrating a new interfacial approach for tuning the interaction between the components aiming at tailoring the performance of the resulting materials, paving the route for their applicability in sustainable packaging.

ASSOCIATED CONTENT

Supporting Information

The Supporting Information is available free of charge at https://pubs.acs.org/doi/10.1021/acs.biomac.9b01733.

Morphological characterization, QCM plots, surface and cross-sectional SEM images, X-ray diffractograms, ATR-FTIR spectra, hydrophobic character of the tannin-containing CNF films, UV−vis spectra, and contents of active compounds and antioxidant activity of tannin extracts (PDF)

AUTHOR INFORMATION

Corresponding Author

Orlando J. Rojas − *Department of Bioproducts and Biosystems, School of Chemical Engineering, Aalto University, Espoo FI-00076, Finland; Departments of Chemical & Biological Engineering, Chemistry, and Wood Science, The University of British Columbia, Vancouver, British Columbia V6T 1Z3, Canada;* orcid.org/0000-0003-4036-4020; Phone: +1 604 822 3457; Email: orlando.rojas@ubc.ca, orlando.rojas@aalto.fi

Authors

André L. Missio − *Laboratório de Produtos Florestais (PPGEF), Centro de Ciências Rurais, Universidade Federal de Santa Maria, Santa Maria, Rio Grande do Sul 97105-900, Brazil*

https://dx.doi.org/10.1021/acs.biomac.9b01733
Biomacromolecules 2020, 21, 1865−1874

Bruno D. Mattos − *Department of Bioproducts and Biosystems, School of Chemical Engineering, Aalto University, Espoo FI-00076, Finland*

Caio G. Otoni − *Department of Bioproducts and Biosystems, School of Chemical Engineering, Aalto University, Espoo FI-00076, Finland;* orcid.org/0000-0001-6734-7381

Marina Gentil − *Laboratório de Produtos Florestais (PPGEF), Centro de Ciências Rurais, Universidade Federal de Santa Maria, Santa Maria, Rio Grande do Sul 97105-900, Brazil*

Rodrigo Coldebella − *Laboratório de Produtos Florestais (PPGEF), Centro de Ciências Rurais, Universidade Federal de Santa Maria, Santa Maria, Rio Grande do Sul 97105-900, Brazil*

Alexey Khakalo − *VTT Technical Research Centre of Finland, Espoo FI-02044 VTT, Finland;* orcid.org/0000-0001-7631-9606

Darci A. Gatto − *Laboratório de Produtos Florestais (PPGEF), Centro de Ciências Rurais, Universidade Federal de Santa Maria, Santa Maria, Rio Grande do Sul 97105-900, Brazil*

Complete contact information is available at: https://pubs.acs.org/10.1021/acs.biomac.9b01733

Author Contributions

⊥A.L.M., B.D.M., and C.G.O. contributed equally.

Notes

The authors declare no competing financial interest.

■ ACKNOWLEDGMENTS

This research was undertaken, in part, thanks to funding from the European Research Council (ERC) under the European Union's Horizon 2020 Research and Innovation Programme (ERC Advanced Grant agreement 788489, "BioElCell") and the Canada Excellence Research Chairs Program (Canada). We are also grateful to the Brazilian National Council for Scientific and Technological Development (CNPQ; Grant 167388/2017-7), the Brazilian Coordination for the Improvement of Higher Education Personnel (CAPES) under the Science Without Borders Program (Grant 88881.068144/2014-01) and Canada Foundation for Innovation.

■ REFERENCES

(1) Mohanty, A. K.; Vivekanandhan, S.; Pin, J.-M.; Misra, M. Composites from Renewable and Sustainable Resources: Challenges and Innovations. *Science (Washington, DC, U. S.)* **2018**, *362* (6414), 536−542.

(2) Geyer, R.; Jambeck, J. R.; Law, K. L. Production, Use, and Fate of All Plastics Ever Made. *Sci. Adv.* **2017**, *3* (7), No. e1700782.

(3) Beurton, J.; Clarot, I.; Stein, J.; Creusot, B.; Marcic, C.; Marchioni, E.; Boudier, A. Long-Lasting and Controlled Antioxidant Property of Immobilized Gold Nanoparticles for Intelligent Packaging. *Colloids Surf., B* **2019**, *176*, 439−448.

(4) Tian, F.; Decker, E. A.; Goddard, J. M. Controlling Lipid Oxidation of Food by Active Packaging Technologies. *Food Funct.* **2013**, *4* (5), 669.

(5) Zheng, J.; Suh, S. Strategies to Reduce the Global Carbon Footprint of Plastics. *Nat. Clim. Change* **2019**, *9* (5), 374−378.

(6) Kontturi, E.; Laaksonen, P.; Linder, M. B.; Nonappa; Gröschel, A. H.; Rojas, O. J.; Ikkala, O. Advanced Materials through Assembly of Nanocelluloses. *Adv. Mater.* **2018**, *30*, 1703779.

(7) Zhu, Y.; Romain, C.; Williams, C. K. Sustainable Polymers from Renewable Resources. *Nature* **2016**, *540* (7633), 354−362.

(8) Farooq, M.; Zou, T.; Riviere, G.; Sipponen, M. H.; Österberg, M. Strong, Ductile, and Waterproof Cellulose Nanofibril Composite Films with Colloidal Lignin Particles. *Biomacromolecules* **2019**, *20* (2), 693−704.

(9) Zhang, Y.; Wang, S.; Xu, W.; Cheng, F.; Pranovich, A.; Smeds, A.; Willför, S.; Xu, C. Valorization of Lignin−Carbohydrate Complexes from Hydrolysates of Norway Spruce: Efficient Separation, Structural Characterization, and Antioxidant Activity. *ACS Sustainable Chem. Eng.* **2019**, *7* (1), 1447−1456.

(10) Li, P.; Sirviö, J. A.; Haapala, A.; Khakalo, A.; Liimatainen, H. Anti-Oxidative and UV-Absorbing Biohybrid Film of Cellulose Nanofibrils and Tannin Extract. *Food Hydrocolloids* **2019**, *92*, 208−217.

(11) Missio, A. L.; Mattos, B. D.; Ferreira, D. de F.; Magalhães, W. L. E.; Bertuol, D. A.; Gatto, D. A.; Petutschnigg, A.; Tondi, G. Nanocellulose-Tannin Films: From Trees to Sustainable Active Packaging. *J. Cleaner Prod.* **2018**, *184*, 143−151.

(12) Hagerman, A. E.; Riedl, K. M.; Jones, G. A.; Sovik, K. N.; Ritchard, N. T.; Hartzfeld, P. W.; Riechel, T. L. High Molecular Weight Plant Polyphenolics (Tannins) as Biological Antioxidants. *J. Agric. Food Chem.* **1998**, *46* (5), 1887−1892.

(13) Widsten, P.; Cruz, C. D.; Fletcher, G. C.; Pajak, M. A.; McGhie, T. K. Tannins and Extracts of Fruit Byproducts: Antibacterial Activity against Foodborne Bacteria and Antioxidant Capacity. *J. Agric. Food Chem.* **2014**, *62* (46), 11146−11156.

(14) Olejar, K. J.; Ray, S.; Ricci, A.; Kilmartin, P. A. Superior Antioxidant Polymer Films Created through the Incorporation of Grape Tannins in Ethyl Cellulose. *Cellulose* **2014**, *21* (6), 4545−4556.

(15) Arbenz, A.; Avérous, L. Chemical Modification of Tannins to Elaborate Aromatic Biobased Macromolecular Architectures. *Green Chem.* **2015**, *17* (5), 2626−2646.

(16) Lourençon, T. V.; Hansel, F. A.; da Silva, T. A.; Ramos, L. P.; de Muniz, G. I. B.; Magalhçes, W. L. E. Hardwood and Softwood Kraft Lignins Fractionation by Simple Sequential Acid Precipitation. *Sep. Purif. Technol.* **2015**, *154*, 82−88.

(17) Missio, A. L.; Tischer, B.; dos Santos, P. S. B.; Codevilla, C.; de Menezes, C. R.; Barin, J. S.; Haselein, C. R.; Labidi, J.; Gatto, D. A.; Petutschnigg, A.; Tondi, G. Analytical Characterization of Purified Mimosa (Acacia Mearnsii) Industrial Tannin Extract: Single and Sequential Fractionation. *Sep. Purif. Technol.* **2017**, *186*, 218−225.

(18) Guo, J.; Tardy, B. L.; Christofferson, A. J.; Dai, Y.; Richardson, J. J.; Zhu, W.; Hu, M.; Ju, Y.; Cui, J.; Dagastine, R. R.; Yarovsky, I.; Caruso, F. Modular Assembly of Superstructures from Polyphenol-Functionalized Building Blocks. *Nat. Nanotechnol.* **2016**, *11*, 1105.

(19) Tardy, B. L.; Yokota, S.; Ago, M.; Xiang, W.; Kondo, T.; Bordes, R.; Rojas, O. J. Nanocellulose−Surfactant Interactions. *Curr. Opin. Colloid Interface Sci.* **2017**, *29*, 57−67.

(20) Ou, B.; Hampsch-Woodill, M.; Prior, R. L. Development and Validation of an Improved Oxygen Radical Absorbance Capacity Assay Using Fluorescein as the Fluorescent Probe. *J. Agric. Food Chem.* **2001**, *49* (10), 4619−4626.

(21) Limaye, M. V.; Schütz, C.; Kriechbaum, K.; Wohlert, J.; Bacsik, Z.; Wohlert, M.; Xia, W.; Pléa, M.; Dembele, C.; Salazar-Alvarez, G.; Bergström, L. Functionalization and Patterning of Nanocellulose Films by Surface-Bound Nanoparticles of Hydrolyzable Tannins and Multivalent Metal Ions. *Nanoscale* **2019**, *11* (41), 19278−19284.

(22) Song, J.; Salas, C.; Rojas, O. J. Role of Textile Substrate Hydrophobicity on the Adsorption of Hydrosoluble Nonionic Block Copolymers. *J. Colloid Interface Sci.* **2015**, *454*, 89−96.

(23) Hatakeyama, T.; Inui, Y.; Iijima, M.; Hatakeyama, H. Bound Water Restrained by Nanocellulose Fibres. *J. Therm. Anal. Calorim.* **2013**, *113* (3), 1019−1025.

(24) Driemeier, C.; Mendes, F. M.; Oliveira, M. M. Dynamic Vapor Sorption and Thermoporometry to Probe Water in Celluloses. *Cellulose* **2012**, *19* (4), 1051−1063.

(25) Mattos, B. D.; Tardy, B. L.; Rojas, O. J. Accounting for Substrate Interactions in the Measurement of the Dimensions of Cellulose Nanofibrils. *Biomacromolecules* **2019**, *20*, 2657.

(26) Carrillo, C. A.; Laine, J.; Rojas, O. J. Microemulsion Systems for Fiber Deconstruction into Cellulose Nanofibrils. *ACS Appl. Mater. Interfaces* **2014**, *6* (24), 22622−22627.

(27) Carrillo, C. A.; Saloni, D.; Rojas, O. J. Evaluation of O/W Microemulsions to Penetrate the Capillary Structure of Woody Biomass: Interplay between Composition and Formulation in Green Processing. *Green Chem.* **2013**, *15* (12), 3377.
(28) Fritz, C.; Ferrer, A.; Salas, C.; Jameel, H.; Rojas, O. J. Interactions between Cellulolytic Enzymes with Native, Autohydrolysis, and Technical Lignins and the Effect of a Polysorbate Amphiphile in Reducing Nonproductive Binding. *Biomacromolecules* **2015**, *16* (12), 3878−3888.
(29) Klockars, K. W.; Tardy, B. L.; Borghei, M.; Tripathi, A.; Garcia Greca, L. G.; Rojas, O. J. Effect of Anisotropy of Cellulose Nanocrystal Suspensions on Stratification, Domain Structure Formation and Structural Colors. *Biomacromolecules* **2018**, *19*, 2931.
(30) Toivonen, M. S.; Onelli, O. D.; Jacucci, G.; Lovikka, V.; Rojas, O. J.; Ikkala, O.; Vignolini, S. Anomalous-Diffusion-Assisted Brightness in White Cellulose Nanofibril Membranes. *Adv. Mater.* **2018**, *30*, 1704050.
(31) Tondi, G.; Petutschnigg, A. Middle Infrared (ATR FT-MIR) Characterization of Industrial Tannin Extracts. *Ind. Crops Prod.* **2015**, *65*, 422−428.
(32) Rojo, E.; Peresin, M. S.; Sampson, W. W.; Hoeger, I. C.; Vartiainen, J.; Laine, J.; Rojas, O. J. Comprehensive Elucidation of the Effect of Residual Lignin on the Physical, Barrier, Mechanical and Surface Properties of Nanocellulose Films. *Green Chem.* **2015**, *17* (3), 1853−1866.
(33) Wang, J.; Gardner, D. J.; Stark, N. M.; Bousfield, D. W.; Tajvidi, M.; Cai, Z. Moisture and Oxygen Barrier Properties of Cellulose Nanomaterial-Based Films. *ACS Sustainable Chem. Eng.* **2018**, *6* (1), 49−70.
(34) Toivonen, M. S.; Kurki-Suonio, S.; Schacher, F. H.; Hietala, S.; Rojas, O. J.; Ikkala, O. Water-Resistant, Transparent Hybrid Nanopaper by Physical Cross-Linking with Chitosan. *Biomacromolecules* **2015**, *16* (3), 1062−1071.
(35) Bedane, A. H.; Eić, M.; Farmahini-Farahani, M.; Xiao, H. Water Vapor Transport Properties of Regenerated Cellulose and Nanofibrillated Cellulose Films. *J. Membr. Sci.* **2015**, *493*, 46−57.
(36) Xiang, W.; Preisig, N.; Laine, C.; Hjelt, T.; Tardy, B. L.; Stubenrauch, C.; Rojas, O. J. Surface Activity and Foaming Capacity of Aggregates Formed between an Anionic Surfactant and Non-Cellulosics Leached from Wood Fibers. *Biomacromolecules* **2019**, *20*, 2286.
(37) Imani, M.; Ghasemian, A.; Dehghani-Firouzabadi, M. R.; Afra, E.; Borghei, M.; Johansson, L. S.; Gane, P. A. C.; Rojas, O. J. Coupling Nanofibril Lateral Size and Residual Lignin to Tailor the Properties of Lignocellulose Films. *Adv. Mater. Interfaces* **2019**, *6* (19), 1900770.
(38) Hsieh, M.-C.; Koga, H.; Suganuma, K.; Nogi, M. Hazy Transparent Cellulose Nanopaper. *Sci. Rep.* **2017**, *7* (1), 41590.
(39) Laghi, L.; Parpinello, G. P.; Rio, D. D.; Calani, L.; Mattioli, A. U.; Versari, A. Fingerprint of Enological Tannins by Multiple Techniques Approach. *Food Chem.* **2010**, *121* (3), 783−788.
(40) Bekbölet, M. Light Effects on Food. *J. Food Prot.* **1990**, *53* (5), 430−440.

https://dx.doi.org/10.1021/acs.biomac.9b01733
Biomacromolecules 2020, 21, 1865−1874